Investigation of buckling behavior of carbon nanotube reinforced nanobeams according to nonlocal elasticity and elastic foundation effects

Karbon nanotüp takviyeli nanokirişlerin burkulma davranışının yerel olmayan elastisite ve elastik zemin etkileriyle incelenmesi

Uğur KAFKAS*[1] (ID), Gökhan GÜÇLÜ[2] (ID)

[1]*Kütahya Dumlupınar University, Vocational School of Technical Science, Department of Construction Technology, 43100, Kütahya*
[2]*Kütahya Dumlupınar University, Engineering Faculty, Department of Civil Engineering, 43100, Kütahya*

Abstract

In this study, the buckling behavior of carbon nanotube (CNT) reinforced nanobeams on an elastic foundation is investigated using the nonlocal elasticity theory and nonlocal finite element method within the framework of Euler-Bernoulli beam theory. The effects of CNT volume fraction, nonlocal parameter, elastic foundation parameter and length-to-thickness ratio on the critical buckling load are analyzed. CNT reinforced nanobeam is modeled considering short and long CNT reinforcements, and mechanical properties are determined by the rule of mixtures. To determine the critical buckling loads of CNT reinforced nanobeams, stiffness matrices and force vectors, including nonlocal effects, are derived based on the Euler-Bernoulli beam theory and analyses are carried out accordingly. The results show that increasing the CNT volume fraction significantly increases the critical buckling load, suggesting that CNTs play an essential role in strengthening the nanobeams. On the other hand, the nonlocal parameter negatively affects the critical buckling load and decreases the buckling strength of the nanobeam. However, the effect of the nonlocal parameter on the buckling strength is negligible. The elastic foundation parameter positively affects the critical buckling load and increases the buckling resistance. This finding indicates that the elastic foundation plays an important role in improving the structural stability of the nanobeams. The length-to-thickness ratio is another important parameter, indicating that long and thin nanobeams are more prone to buckling and the critical buckling load decreases with increasing this ratio. Since the effects of the above-mentioned four parameters on the buckling strength were determined using the finite element method, the results obtained will guide the subsequent numerical modeling studies of nano-sized beams.

Keywords: Carbon nanotube (CNT) reinforced nanobeams, Critical buckling load, Elastic foundation parameter, Finite element method, Nonlocal elasticity theory

Öz

Bu çalışmada, elastik bir zemin üzerinde yer alan karbon nanotüp (KNT) takviyeli nanokirişlerin burkulma davranışı, Euler-Bernoulli kiriş teorisi çerçevesinde yerel olmayan elastisite teorisi ve yerel olmayan sonlu elemanlar yöntemi kullanılarak incelenmiştir. KNT hacim oranı, yerel olmayan parametre, elastik zemin parametresi ve uzunluk/kesit kalınlığı oranı gibi parametrelerin kritik burkulma yükü üzerindeki etkileri analiz edilmiştir. Kısa ve uzun KNT takviyeleri dikkate alınarak KNT takviyeli nanokiriş modellenmiş ve mekanik özellikler karışım kuramı kullanılarak belirlenmiştir. KNT takviyeli nanokirişlerin kritik burkulma yüklerinin belirlenebilmesi amacıyla, Euler-Bernoulli kiriş teorisine dayalı olarak yerel olmayan etkileri de içeren rijitlik matrisleri ve kuvvet vektörleri türetilmiş ve analizler bu doğrultuda gerçekleştirilmiştir. Sonuçlar, KNT hacim oranının artmasının kritik burkulma yükünü önemli ölçüde artırdığını göstermektedir, bu da KNT'lerin nanokirişleri güçlendirmede önemli bir rol oynadığını ortaya koymaktadır. Diğer yandan, yerel olmayan parametre kritik burkulma yükünü olumsuz etkilemekte ve nanokirişin burkulma dayanımını azaltmaktadır. Ancak yerel olmayan parametrenin burkulma dayanımına olan etkisi ihmal edilebilir düzeydedir. Elastik zemin parametresi ise kritik burkulma yükünü pozitif yönde etkilemekte olup, burkulma direncini artırmaktadır. Bu bulgu, elastik zeminin nanokirişlerin yapısal stabilitesini geliştirmede önemli bir rol oynadığını göstermektedir. Uzunluk/kesit kalınlığı oranı da bir diğer önemli parametre olup, uzun ve ince nanokirişlerin burkulmaya daha yatkın olduğunu ve bu oranın artmasıyla birlikte kritik burkulma yükünün azaldığını göstermektedir. Yukarıda belirtilen dört parametrenin burkulma dayanımına olan etkisi sonlu elemanlar yöntemi kullanılarak belirlendiği için bundan sonraki nano boyutlu kirişlerin sayısal olarak modellenmesi çalışmalarında elde edilen sonuçlar yol gösterici olacaktır.

Anahtar kelimeler: *Karbon nanotüp (KNT) takviyeli nanokirişler, Kritik burkulma yükü, Elastik zemin parametresi, Sonlu elemanlar yöntemi, Yerel olmayan elastisite teorisi*

*Uğur KAFKAS; ugur.kafkas@dpu.edu.tr

1. Introduction

Carbon nanotube (CNT) reinforced nanobeams have become an important research topic in nanotechnology and advanced materials science. The extraordinary mechanical properties of these nanomaterials are of great interest, especially in terms of key parameters that determine the durability of structures, such as critical buckling loads (Arshid et al., 2021). The high strength-to-weight ratio of carbon nanotubes makes them ideal reinforcement materials for composite structures (Suhr et al., 2005; Namilae & Chandra, 2006). With CNT reinforcement, nanoscale structures can exhibit significantly improved mechanical performance and lighter structures can be designed with higher load-carrying capacity (Pouresmaeeli & Fazelzadeh, 2017; Lal & Markad, 2019). CNT reinforced nanomaterials also play an essential role in energy storage devices. They are used primarily in lithium-ion batteries and supercapacitors to increase energy density and ensure durability in charge/discharge cycles (Baughman et al., 2002). In addition, CNT reinforced materials are used in sensor technology, especially in chemical and biological sensing systems; high sensitivity and fast response times are among the most essential advantages of these materials (Balasubramanian & Burghard, 2005). CNT reinforced nanobeams have been used in various industries due to their high strength, lightweight, and excellent mechanical properties. In particular, they are used in the aerospace and automotive sectors to produce more durable and lightweight composite materials (Esawi & El Borady, 2008). They are also used as microactuators and microresonators with low stiffness and high vibration frequencies in nano-electromechanical systems (NEMS) and micro-mechanical systems (MEMS) (Ashrafi et al., 2006). However, a complete understanding of the mechanical behavior of nanostructures still presents several challenges, especially in terms of prediction and control of unstable behavior such as buckling (Wang et al., 2007; Motevalli et al., 2012). Understanding the buckling behavior of nano-sized beams plays a critical role in predicting the performance of materials at nanoscales. In this context, buckling analyses of CNT reinforced nanobeams go beyond classical beam theories and include phenomena occurring at the nano level, such as quantum effects and size effects (Wattanasakulpong & Ungbhakorn, 2013). However, the exact modeling of buckling behavior in such beams is quite complex due to the heterogeneous structure of the material and the anisotropic properties of CNTs (Thang, 2019). In addition, such structures are usually located on an elastic medium such as soil, which can significantly affect the buckling behavior of the structures (Pradhan & Reddy, 2011; Yaylı, 2017). This study investigates the buckling behavior of CNT reinforced nanobeams resting on a Winkler-type elastic foundation.

The Winkler-type elastic foundation model is a common technique that models soil effects with a simplified approach. In this model, the soil is represented as independent springs placed under each unit area and the stiffness coefficient of these springs depends on the properties of the foundation. Winkler-type elastic foundations consider the soil-beam interaction, which is an important parameter affecting the buckling behavior of structures (Pradhan & Reddy, 2011). It is thought that the buckling analysis of CNT reinforced nanobeams on an elastic soil will produce important results that will allow the determination of the necessary design parameters to optimize the safety and performance of structures (Thang, 2019). Considering the anisotropic properties of soil and CNTs together allows the design parameters of these structures to be determined more accurately (Setoodeh et al., 2015).

Classical beam theories are generally valid for micro- and macro-scale structures and insufficient for analyzing nanoscale structures. More precise modeling of mechanical behaviors occurring in nanobeams requires advanced approaches such as nonlocal elasticity theory (Yaylı, 2019). Nonlocal elasticity theory reflects materials' stress and deformation behaviors at the nanoscale more realistically by considering long-range interactions between material points (Taghizadeh et al., 2016). In this context, nonlocal elasticity theory offers a more comprehensive approach than classical elasticity theories and plays an essential role in buckling analysis on nanoscale structures (Phadikar & Pradhan, 2010). Non-classical elasticity theories are not limited to nonlocal elasticity theory. There are many other theories. Some of them are: couple stress theory (Toupin, 1962), micropolar theory (Eringen, 1967), modified couple stress theory (Yang et al., 2002), modified strain gradient theory (Lam et al., 2003), nonlocal strain gradient theory (Lim et al., 2015), second strain gradient theory (Mindlin, 1965), strain gradient theory (Aifantis, 1999), surface elasticity theory (Gurtin et al., 1998).

The finite element method is widely used for the numerical solution of complex engineering problems. This method is based on a piecewise approach to simulate the mechanics of structures and predicts the behavior of the entire structure based on the solution of each element (Taghizadeh et al., 2016). The method has been extensively employed in macro- to micro- and nano-scales analyses. Numerous scholarly works document its

application to both static and dynamic examinations of beam structures—encompassing bending, buckling, and vibration—across these dimensional ranges. The finite element method is widely used in macro-scale for bending (Uhm & Youn, 2009; Kahya & Turan, 2017; Reddy et al., 2020; Song et al., 2022; Chi Tho et al., 2023), vibration (Dai & Liu, 2007; Turan & Kahya, 2018; Pham et al., 2022; Bentrar et al., 2023; Turan & Hacıoğlu, 2023; Zhu et al., 2024) and buckling (Casafont et al., 2009; Feng et al., 2015; Turan & Kahya, 2021; Turan & Hacıoğlu, 2022; Yaylacı et al., 2023; Mesbah et al., 2023) problems. At the micro/nanoscale, the finite element method has been widely employed to investigate both static and dynamic responses in nano-scale beam-type elements, including static bending (Demir et al., 2018; Uzun & Yaylı, 2022; Kafkas, 2024), vibration (Eltaher et al., 2013; Uzun et al., 2018; Civalek & Numanoğlu, 2020; Civalek et al., 2020a; Karamanli & Vo, 2022; Uzun et al., 2020; Uzun et al., 2021) and buckling (Tuna & Kirca, 2017; Aria & Friswell, 2019; Belarbi et al., 2021), within the framework of diverse theoretical models. The finite element method for the analysis of nanobeams is a powerful tool to account for the heterogeneous structure of materials, dimensional effects, and the effects of elastic foundation (Civalek et al., 2020b). By integrating the theory of nonlocal elasticity into the finite element method, many problems that cannot be solved analytically can be solved numerically. However, it can be stated that the classical analysis results are a special case of this formulation; therefore, the nonlocal theory offers a more general formulation. In addition, investigating the effects of nonlocal parameters and CNT reinforcement ratios is very important regarding material design and optimization (Wu & Yu, 2019).

The nonlocal finite element method used in this study allows the determination of nanobeam buckling loads using the numerical solution method. The main objective of this study is to investigate the buckling behavior of CNT reinforced nanobeams on an elastic foundation and to determine the critical buckling loads. The effects of various parameters such as CNT reinforcement type, CNT volume fraction, Winkler-type elastic foundation parameter and nonlocal parameter on buckling loads are investigated in the study. While CNT reinforcement improves the mechanical performance of nanobeams, the effect of nonlocal parameters is essential in modeling the size effects on nanoscale structures. Moreover, the elastic foundation parameter affects the buckling behavior by considering the interactions with the soil beneath the beam. Each of these parameters is a critical factor to consider in the design and analysis of nanostructures. In the reviewed part of the literature, no study examined the effect of the specified parameters on the buckling strength of CNT reinforced nanobeams. In this study, since it was determined to what extent the parameters examined affect the buckling strength, the results obtained are expected to guide the stability analysis of nanobeams. In addition, the results obtained by taking the elastic foundation parameter as zero can also be used for nanobeams that do not rest on elastic foundations.

2. Material and method

2.1. Determination of material properties of CNT reinforced nanobeams

In this study, determining material properties and predicting mechanical properties such as modulus of elasticity and shear modulus, necessary to understand the buckling behavior of CNT reinforced nanobeams, are based on the rule of mixtures and various scale-dependent parameters. Depending on the lengths and volume ratios of carbon nanotubes, the elastic properties of the materials change significantly.

Figure 1 shows the schematic representation of a short (10,10) and long (10,10) single-walled carbon nanotube (SWCNT) reinforced simply supported nanobeam resting on a Winkler-type elastic foundation. Here, the numbers (10,10) represent the projections of the vectors in the atomic arrangement in the schematic structure of the carbon nanotube in a specific direction. The cross-section of the nanobeam with the beam axis as the x-axis is also shown. The length of the beam is denoted by L, compressive axial force by N and the cross-sectional dimensions are denoted by b and h.
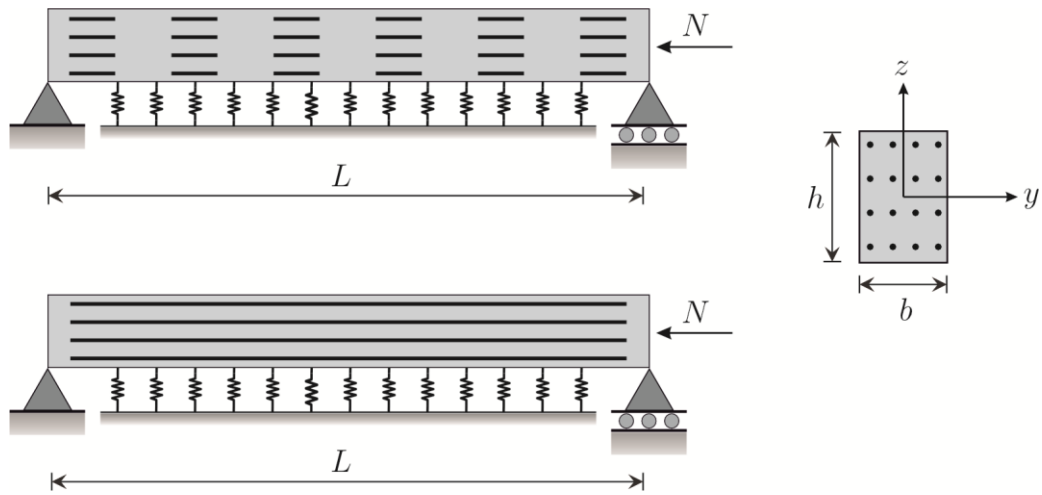
Figure 1. Short and long SWCNT reinforced nanobeam

The formulas used in this study are based on the assumption that CNT reinforced composites exhibit isotropic behavior. Based on the rule of mixture, the longitudinal elastic modulus of CNT reinforced composites can be calculated with the following formula (Shen, 2009):

$$E_{11} = \zeta_1 V_{CNT} E_{11}^{CNT} + V_m E^m \tag{1}$$

Here, E_{11} represents the longitudinal elastic modulus of CNT reinforced nanomaterial, ζ_1 is the carbon nanotube efficiency parameter, while V_{CNT} and V_m represent the volume fractions of carbon nanotube and matrix, respectively. E_{11}^{CNT} is the longitudinal elastic modulus of carbon nanotube and E^m represents the elastic modulus of isotropic matrix material.

At the same time, the transverse elastic modulus of CNT reinforced nanobeam is calculated as follows (Fattahi & Safaei, 2017):

$$E_{22} = \frac{\zeta_2}{\left(\dfrac{V_{CNT}}{E_{22}^{CNT}} + \dfrac{V_m}{E^m}\right)} \tag{2}$$

Here E_{22} and E_{22}^{CNT} represent the transverse elastic modulus of CNT reinforced nanobeam and the transverse elastic modulus of carbon nanotube, respectively. The volume fractions are related by the equation $V_{CNT} + V_m = 1$. The ζ_2 used in the formula is the carbon nanotube efficiency parameter reflecting scale-dependent material properties. These parameters were obtained by Fattahi and Safaei (2017) using molecular dynamics simulation corresponding to both short (10,10) and long (10,10) SWCNT composites embedded with amorphous polyethylene matrix, and these data are also used in this study. The relevant data are given in tabular form in Table 1.

Table 1. CNT efficiency parameters (Fattahi & Safaei, 2017)

V_{CNT}	ζ_1	ζ_2
Short CNT-reinforced		
5%	0.0254	1.0351
10%	0.0443	1.2854
15%	0.0628	1.7798
25%	0.0740	1.8751
Long CNT-reinforced		
5%	2.1577	1.1767
10%	1.6354	1.4765
15%	1.6868	2.0588
25%	1.6531	2.1820

2.2. Obtaining finite element matrices for buckling problem

The Euler-Bernoulli beam theory (EBT) is a classical theory used to analyze the bending behavior of a beam. The buckling problem analyzes the stability of the beam under the effect of axial compressive force N. In this section, stiffness matrices and force vectors of finite element analysis will be given. In particular, under axial compressive force and together with the Winkler-type elastic foundation parameter (k), the nonlocal elasticity theory is also included in this analysis.

According to the nonlocal elasticity theory, Hooke's law for linear, isotropic and elastic bodies in the case of uniaxial deformation is given by (Wang et al., 2006):

$$\sigma(x) - \mu \frac{d^2 \sigma(x)}{dx^2} = E_{11} \varepsilon(x) \tag{3}$$

Here, σ is the nonlocal stress, ε is the nonlocal strain and μ is the nonlocal parameter from the nonlocal elasticity theory. The free body diagram of the differential length of the nanobeam is given Figure 2.
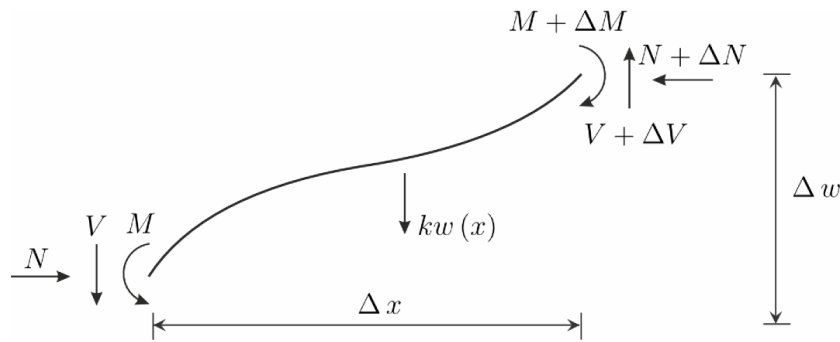

Figure 2. Free body diagram of the differential length of the nanobeam

By writing equilibrium equations for moments and forces in the transverse direction and then taking the limit of these equations

$$\frac{dV}{dx} = kw(x) \tag{4}$$

$$\frac{dM}{dx} = V + N \frac{dw}{dx} \tag{5}$$

identities are obtained. Here, w is the transverse displacement, V is the shear force and M is the bending moment. The bending moment and axial strain are calculated from

$$M = \int_A z\sigma dA \tag{6}$$

$$\varepsilon = -z \frac{d^2 w}{dx^2} \tag{7}$$

Substituting equation (6) and (7) into equation (3) gives

$$M - \mu \frac{d^2 M}{dx^2} = -E_{11} I \frac{d^2 w}{dx^2} \tag{8}$$

Here I is the moment of inertia of the nanobeam. Equation (8) is the nonlocal constitutive equation of the nanobeam. By taking the derivative of equation (5) with respect to x and using equation (4)

$$\frac{d^2M}{dx^2} = \frac{dV}{dx} + N\frac{d^2w}{dx^2} = kw + N\frac{d^2w}{dx^2} \tag{9}$$

is obtained. Taking second order derivative of equation (8) and using equation (9) leads to

$$\frac{d^2M}{dx^2} = \mu\frac{d^4M}{dx^4} - E_{11}I\frac{d^4w}{dx^4} = \mu\left(k\frac{d^2w}{dx^2} + N\frac{d^4w}{dx^4}\right) - E_{11}I\frac{d^4w}{dx^4} \tag{10}$$

Equating the right sides of equations (9) and (10) gives

$$E_{11}I\frac{d^4w}{dx^4} + kw - \mu k\frac{d^2w}{dx^2} + N\frac{d^2w}{dx^2} - \mu N\frac{d^4w}{dx^4} = 0 \tag{11}$$

the governing differential equation for buckling of the nanobeam rests on the Winkler-type elastic foundation.

The analytical solution of equation (11) for the simply supported nanobeam will be obtained. The boundary conditions for this case are given as

$$w(0) = M(0) = w(L) = M(L) = 0 \tag{12}$$

To satisfy the given boundary conditions in equation (11), the transverse displacement function $w(x)$ is expressed by the

$$w(x) = \sum_{n=1}^{\infty} W_n \sin\frac{n\pi x}{L} \tag{13}$$

half-range Fourier sine series expansion. Here W_n are the Fourier coefficients. By substituting equation (13) in equation (11)

$$\sum_{n=1}^{\infty}\left(k + \frac{n^2\pi^2 k\mu}{L^2} + \frac{n^4\pi^4 E_{11}I}{L^4} - \frac{n^4\pi^4\mu N}{L^4} - \frac{n^2\pi^2 N}{L^2}\right)W_n\sin\frac{\pi n x}{L} = 0 \tag{14}$$

is obtained. To satisfy equation (14) in the $0 < x < L$ interval, which is the domain of the differential equation (11), coefficients of every $W_n\sin\pi n x/L$ term in equation (14) should be equal to zero, which gives

$$k + \frac{n^2\pi^2 k\mu}{L^2} + \frac{n^4\pi^4 E_{11}I}{L^4} - \frac{n^4\pi^4\mu N}{L^4} - \frac{n^2\pi^2 N}{L^2} = 0, \qquad n \geq 1 \tag{15}$$

condition. By arranging equation (15), one obtains the critical buckling loads of the nanobeam:

$$N_{cr}^n = \frac{n^2\pi^2(\mu k\,L^2 + n^2\pi^2 E_{11}I) + kL^4}{n^2\pi^2(L^2 + n^2\pi^2\mu)}, \qquad n \geq 1 \tag{16}$$

Here, N_{cr}^n is the critical buckling load of the nanobeam for the nth mode.

2.3. Galerkin finite element formulation

Analytical solutions cannot be obtained in many cases due to the complexity of the governing equation(s), boundary condition(s), or the domain of the problem. The analytical solution is not in closed form, which is where they can be obtained in most cases. In the finite element method, the domain of the problem is divided into subdomains. According to the variational approximation method used, the governing equation's weighted integral form is satisfied on each subdomain. Thus, the problem's solution is transformed from the solution of the differential equation(s) to the solution of the system of algebraic equations. The algebraic equations obtained for each subdomain are combined using the conditions of continuity of the primary variables and

equilibrium of the secondary variables at the relevant nodes. The values of the primary and secondary variables are determined by solving the algebraic equation set of the entire system. The value of the primary variable at any point in the domain of the problem is determined by taking the linear combination of the shape functions and the primary variable values obtained at the nodes. The finite element method can numerically solve almost all engineering problems encountered. It is the most common and general numerical solution method in engineering fields.

The finite element formulation is obtained using the weak-form Galerkin (Ritz) variational approximation method. The beam is analyzed by dividing it into small elements along its length. Nodes are assigned to the start and end points of each element. Since each node has two degrees of freedom (transverse deflection and rotation), each element's total degree of freedom is 4. These freedoms consist of the nodal generalized displacements $w_1, \theta_1, w_2, \theta_2$ which are elements of the generalized displacement vector $\mathbf{u} = [w_1 \quad \theta_1 \quad w_2 \quad \theta_2]^T$. The shape function vector $\boldsymbol{\varphi}$ of the beam, with the length of each element being l_e, is given as follows (Reddy, 2002):

$$\boldsymbol{\varphi} = \left[1 - \frac{3x^2}{l_e^2} + \frac{2x^3}{l_e^3} \quad x - \frac{2x^2}{l_e} + \frac{x^3}{l_e^2} \quad \frac{3x^2}{l_e^2} - \frac{2x^3}{l_e^3} \quad -\frac{x^2}{l_e} + \frac{x^3}{l_e^2}\right] \tag{17}$$

The approximate transverse deflection of the nanobeam can be expressed as follows:

$$w_N = \boldsymbol{\varphi}\mathbf{u} = \varphi_1 w_1 + \varphi_2 \theta_1 + \varphi_3 w_2 + \varphi_4 \theta_2 \tag{18}$$

According to the theory of nonlocal elasticity, including the Winkler-type elastic foundation effect, to obtain the weak form of the governing differential equation for buckling, the Z residual can be expressed as follows:

$$Z = E_{11}I\frac{d^4 w_N}{dx^4} + kw_N - \mu k\frac{d^2 w_N}{dx^2} + N\frac{d^2 w_N}{dx^2} - \mu N\frac{d^4 w_N}{dx^4} \tag{19}$$

To determine the weighted integral form of the differential equation, the shape functions φ_i are chosen as weight functions, the Z residual is multiplied by the weight functions and the resulting expression is integrated over the length of the nanobeam:

$$\int_0^L \left(\boldsymbol{\varphi}^T E_{11}I\frac{d^4 w_N}{dx^4} + \boldsymbol{\varphi}^T kw_N - \boldsymbol{\varphi}^T \mu k\frac{d^2 w_N}{dx^2} + \boldsymbol{\varphi}^T N\frac{d^2 w_N}{dx^2} - \boldsymbol{\varphi}^T \mu N\frac{d^4 w_N}{dx^4}\right) dx = 0 \tag{20}$$

Applying the partial integration twice in equation (20) (this is Ritz formulation, also known as weak-form Galerkin formulation), the general form can be written as follows:

$$\int_0^L \left(E_{11}I\frac{d^2\boldsymbol{\varphi}^T}{dx^2}\frac{d^2\boldsymbol{\varphi}}{dx^2} + k\boldsymbol{\varphi}^T\boldsymbol{\varphi} + \mu k\frac{d\boldsymbol{\varphi}^T}{dx}\frac{d\boldsymbol{\varphi}}{dx} - N\frac{d\boldsymbol{\varphi}^T}{dx}\frac{d\boldsymbol{\varphi}}{dx} - \mu N\frac{d^2\boldsymbol{\varphi}^T}{dx^2}\frac{d^2\boldsymbol{\varphi}}{dx^2}\right)\mathbf{u}dx$$
$$+ \left(E_{11}I\boldsymbol{\varphi}^T\frac{d^3\boldsymbol{\varphi}\mathbf{u}}{dx^3}\right)\Big|_{x=0}^L - \left(E_{11}I\frac{d\boldsymbol{\varphi}^T}{dx}\frac{d^2\boldsymbol{\varphi}\mathbf{u}}{dx^2}\right)\Big|_{x=0}^L - \left(\mu k\boldsymbol{\varphi}^T\frac{d\boldsymbol{\varphi}\mathbf{u}}{dx}\right)\Big|_{x=0}^L + \left(N\boldsymbol{\varphi}^T\frac{d\boldsymbol{\varphi}\mathbf{u}}{dx}\right)\Big|_{x=0}^L$$
$$- \left(\mu N\boldsymbol{\varphi}^T\frac{d^3\boldsymbol{\varphi}\mathbf{u}}{dx^3}\right)\Big|_{x=0}^L + \left(\mu N\frac{d\boldsymbol{\varphi}^T}{dx}\frac{d^2\boldsymbol{\varphi}\mathbf{u}}{dx^2}\right)\Big|_{x=0}^L = 0 \tag{21}$$

The stiffness and buckling load matrices of the CNT reinforced nanobeam are obtained by substituting the shape functions in equation (17) into equation (21) and taking the integrals one by one. These matrices are defined as follows:

$$\mathbf{K}_E = E_{11}I\int_0^{l_e} \begin{Bmatrix} \varphi_1'' \\ \varphi_2'' \\ \varphi_3'' \\ \varphi_4'' \end{Bmatrix} \{\varphi_1'' \quad \varphi_2'' \quad \varphi_3'' \quad \varphi_4''\}dx = \frac{E_{11}I}{l_e^3}\begin{bmatrix} 12 & 6l_e & -12 & 6l_e \\ 6l_e & 4l_e^2 & -6l_e & 2l_e^2 \\ -12 & -6l_e & 12 & -6l_e \\ 6l_e & 2l_e^2 & -6l_e & 4l_e^2 \end{bmatrix} \tag{22}$$

$$\mathbf{K}_{k1} = k \int_0^{l_e} \begin{Bmatrix} \varphi_1 \\ \varphi_2 \\ \varphi_3 \\ \varphi_4 \end{Bmatrix} \{\varphi_1 \quad \varphi_2 \quad \varphi_3 \quad \varphi_4\} dx = \frac{k}{420} \begin{bmatrix} 156l_e & 22l_e^2 & 54l_e & -13l_e^2 \\ 22l_e^2 & 4l_e^3 & 13l_e^2 & -3l_e^3 \\ 54l_e & 13l_e^2 & 156l_e & -22l_e^2 \\ -13l_e^2 & -3l_e^3 & -22l_e^2 & 4l_e^3 \end{bmatrix} \tag{23}$$

$$\mathbf{K}_{k2} = \mu k \int_0^{l_e} \begin{Bmatrix} \varphi_1' \\ \varphi_2' \\ \varphi_3' \\ \varphi_4' \end{Bmatrix} \{\varphi_1' \quad \varphi_2' \quad \varphi_3' \quad \varphi_4'\} dx = \frac{\mu k}{30l_e} \begin{bmatrix} 36 & 3l_e & -36 & 3l_e \\ 3l_e & 4l_e^2 & -3l_e & -l_e^2 \\ -36 & -3l_e & 36 & -3l_e \\ 3l_e & -l_e^2 & -3l_e & 4l_e^2 \end{bmatrix} \tag{24}$$

$$\mathbf{B}_{N1} = N \int_0^{l_e} \begin{Bmatrix} \varphi_1' \\ \varphi_2' \\ \varphi_3' \\ \varphi_4' \end{Bmatrix} \{\varphi_1' \quad \varphi_2' \quad \varphi_3' \quad \varphi_4'\} dx = \frac{N}{30l_e} \begin{bmatrix} 36 & 3l_e & -36 & 3l_e \\ 3l_e & 4l_e^2 & -3l_e & -l_e^2 \\ -36 & -3l_e & 36 & -3l_e \\ 3l_e & -l_e^2 & -3l_e & 4l_e^2 \end{bmatrix} \tag{25}$$

$$\mathbf{B}_{N2} = \mu N \int_0^{l_e} \begin{Bmatrix} \varphi_1'' \\ \varphi_2'' \\ \varphi_3'' \\ \varphi_4'' \end{Bmatrix} \{\varphi_1'' \quad \varphi_2'' \quad \varphi_3'' \quad \varphi_4''\} dx = \frac{\mu N}{l_e^3} \begin{bmatrix} 12 & 6l_e & -12 & 6l_e \\ 6l_e & 4l_e^2 & -6l_e & 2l_e^2 \\ -12 & -6l_e & 12 & -6l_e \\ 6l_e & 2l_e^2 & -6l_e & 4l_e^2 \end{bmatrix} \tag{26}$$

As can be understood from here, the system stiffness matrix is $\mathbf{K} = \mathbf{K}_E + \mathbf{K}_{k1} + \mathbf{K}_{k2}$ and $\mathbf{B} = \mathbf{B}_{N1} + \mathbf{B}_{N2}$ is the force vector, the critical buckling load is obtained by solving the following eigenvalue problem (Phadikar & Pradhan, 2010):

$$|\mathbf{K} - \lambda \mathbf{B}| = 0 \tag{27}$$

$$\lambda = \frac{N}{N_{cr}} \tag{28}$$

Here N_{cr} represents the critical buckling load.

3. Results and discussion

This section investigates the effects of different parameters on the buckling behavior of CNT reinforced nanobeams. An analysis will be made for the buckling performance of nanobeams using variables such as nonlocal parameter, elastic foundation parameter, beam length-to-thickness ratio and CNT volume fraction. The calculations made for short and long CNT reinforced nanobeam models with different CNT volume fractions will be evaluated in detail by considering various foundation stiffnesses and beam geometries. The effects of these parameters on the buckling strength and stiffness of nanobeams will be explained with the help of tables and figures.

The elastic foundation is a parameter that directly affects the stability and buckling behavior of the beam and is used to model the effects of foundation stiffness on the beam. The elastic foundation parameter k is based on a Winkler-type foundation model and represents the force required for the foundation to make a unit displacement corresponding to the displacements at different points of the beam. The dimensionless parameter K_W is expressed by the following formula:

$$K_W = \frac{kL^4}{E_{11}I} \tag{29}$$

The nanobeam analyzed in this study is manufactured from CNT reinforced composite material. In particular, SWCNTs with (10,10) armchair structure and a polyethylene matrix with isotropic behavior are used. The properties of the nanobeam obtained by combining these two materials are based on data from the literature. The elasticity modulus of the polyethylene matrix is taken as $E^m = 3.22$ GPa at room temperature and the

elasticity modulus of the (10,10) armchair SWCNT used as carbon nanotube reinforcement was taken as $E_{11}^{CNT} = 600$ GPa and $E_{22}^{CNT} = 10$ GPa (Popov et al., 2000; Fattahi & Safaei, 2017).

These properties define the mechanical behavior of SWCNT and the effective elasticity and shear moduli of the nanobeam are calculated using the rule of mixtures. The CNT volume fractions during the calculations were taken as $V_{CNT} = 0.05, 0.10, 0.15$ and 0.25. Throughout the study, beam cross-sectional dimensions are taken as $b = h = 10$ nm. In cases where the L/h ratio is 10 and above, the contribution of shear deformations to the strain energy remains below 5%. In this study, Euler-Bernoulli beam theory is used since solutions are obtained for $L/h = 10$.

Table 2 presents the N_{cr} values obtained from the exact solution in this study and given in Equation (16), and the finite element models using different numbers of elements (N^e). For this comparison study, $V_{CNT} = 0$ and the beam parameters are set as $K_W = 10$, $E_{11} = E^m = 3.22$ GPa, $\mu = 1$, and $\frac{L}{h} = 10$.

Table 2. Comparison of the first 5 modes N_{cr} values (N) for a simply supported nanobeam

Mode	Eq. (16)	FEM Eq. (27)					
		$N^e = 5$	$N^e = 10$	$N^e = 15$	$N^e = 20$	$N^e = 25$	$N^e = 30$
1	2.9176	2.9182	2.9176	2.9176	2.9176	2.9176	2.9176
2	10.6197	10.6534	10.6219	10.6201	10.6198	10.6197	10.6197
3	23.6554	24.0040	23.6800	23.6604	23.6570	23.6561	23.6558
4	41.7318	43.4329	41.8634	41.7588	41.7408	41.7354	41.7335
5	64.6252	78.1660	65.0994	64.7327	64.5538	64.6384	64.6316

The results in Table 2 show that the finite element solution given in Eq. (27) closely matches the analytical solution. The first mode frequencies show a remarkable agreement for all finite element models, confirming the accuracy of the finite element model for low buckling modes. For higher modes, slight discrepancies are observed when fewer elements are used. However, these differences decrease significantly as the number of elements increases in the finite element model. In this study, $N^e = 30$ is taken for the finite element models.

Tables 3-4 and Figures 3-4 show the effects of nonlocal parameters and CNT volume fractions on the critical buckling load for short and long CNT reinforced nanobeams. $K_W = 10$ and $\frac{L}{h} = 10$ values are used during the analysis.

Table 3. N_{cr} values (N) of short CNT reinforced nanobeam for different μ and V_{CNT} parameters

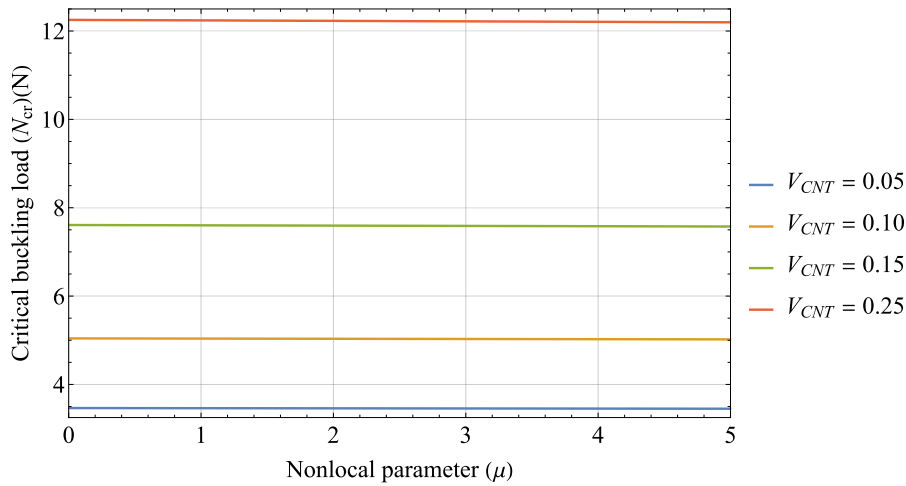| V_{CNT}	μ (nm²)									
	0	0.1	0.5	1	1.5	2	2.5	3	4	5
5%	3.465	3.465	3.464	3.462	3.461	3.459	3.458	3.456	3.453	3.450
10%	5.042	5.042	5.040	5.038	5.036	5.033	5.031	5.029	5.024	5.020
15%	7.609	7.608	7.605	7.602	7.599	7.595	7.592	7.589	7.582	7.575
25%	12.252	12.251	12.247	12.241	12.236	12.230	12.225	12.219	12.209	12.198

Figure 3. N_{cr} values of short CNT reinforced nanobeam for different μ and V_{CNT} parameters

Table 4. N_{cr} values (N) of long CNT reinforced nanobeam for different μ and V_{CNT} parameters

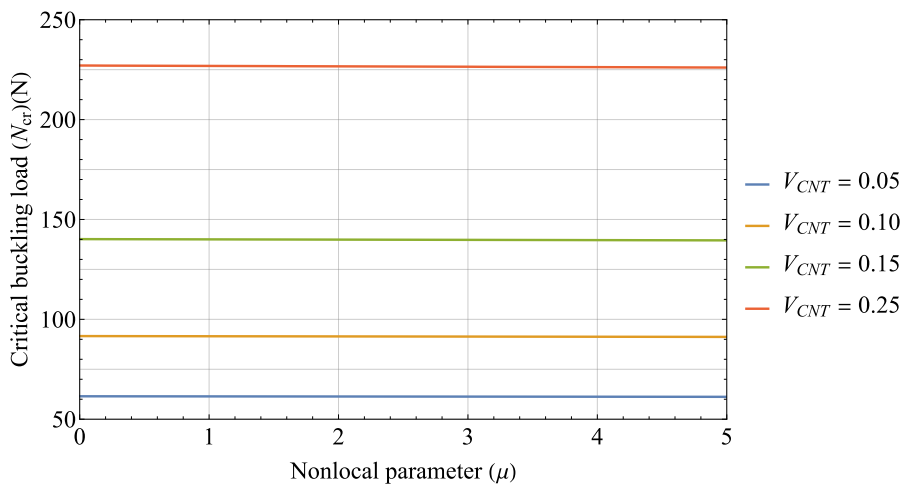| V_{CNT}	μ (nm^2)									
	0	0.1	0.5	1	1.5	2	2.5	3	4	5
5%	61.479	61.473	61.451	61.424	61.396	61.369	61.342	61.314	61.260	61.205
10%	91.615	91.607	91.574	91.533	91.492	91.451	91.411	91.370	91.288	91.207
15%	140.162	140.149	140.099	140.036	139.974	139.911	139.849	139.786	139.662	139.537
25%	227.070	227.050	226.968	226.867	226.766	226.664	226.563	226.462	226.260	226.059

Figure 4: N_{cr} values of long CNT reinforced nanobeam for different μ and V_{CNT} parameters

Tables 3-4 and Figures 3-4 show that the critical buckling load increases significantly as the CNT volume fraction increases regardless of whether long or short CNT reinforcement is used. This shows that CNT reinforcement increases the stiffness and buckling strength of the nanobeam. This increase is slightly higher for long CNT reinforced nanobeams. As the nonlocal parameter increases, the critical buckling load decreases, but this decrease is almost imperceptible. This means that the nonlocal parameter does not affect the buckling load. The resulting formulation is more complex when the nonlocal elasticity theory is used in the beam model. Still, the effect of the nonlocal parameter on the buckling load is almost negligible. Therefore, there is no need to use nonlocal elasticity theory in the beam model.

Tables 5-6 and Figures 5-6 show the effects of dimensionless elastic foundation parameters and CNT volume fractions on the critical buckling load for short and long CNT reinforced nanobeams. $\mu = 0.5$ and $\frac{L}{h} = 10$ values are used during the analysis.

Table 5. N_{cr} values (N) of short CNT reinforced nanobeam for different K_W and V_{CNT} parameters

V_{CNT}	K_W								
	0	1	2	3	4	5	10	20	50
5%	3.141	3.173	3.206	3.238	3.270	3.302	3.464	3.786	4.754
10%	4.571	4.618	4.665	4.711	4.758	4.805	5.040	5.510	6.918
15%	6.897	6.968	7.039	7.110	7.180	7.251	7.605	8.314	10.439
25%	11.106	11.220	11.334	11.448	11.562	11.676	12.247	13.387	16.810
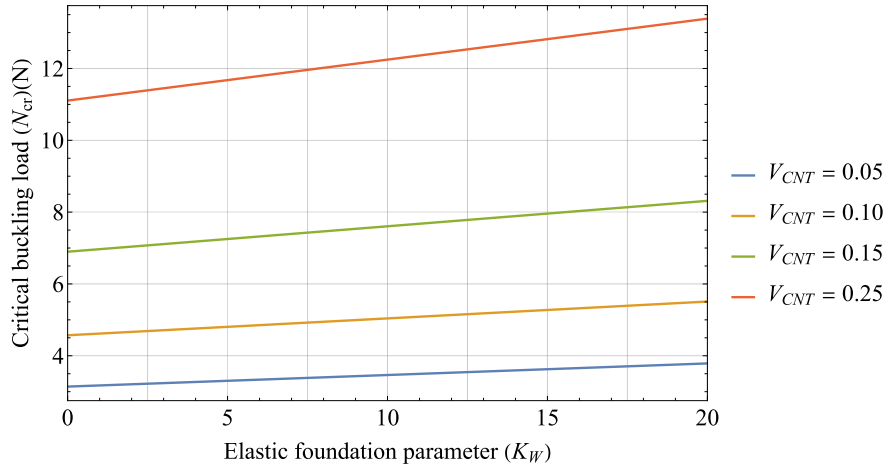
Figure 5. N_{cr} values of short CNT reinforced nanobeam for different K_W and V_{CNT} parameters

Table 6. N_{cr} values (N) of long CNT reinforced nanobeam for different K_W and V_{CNT} parameters

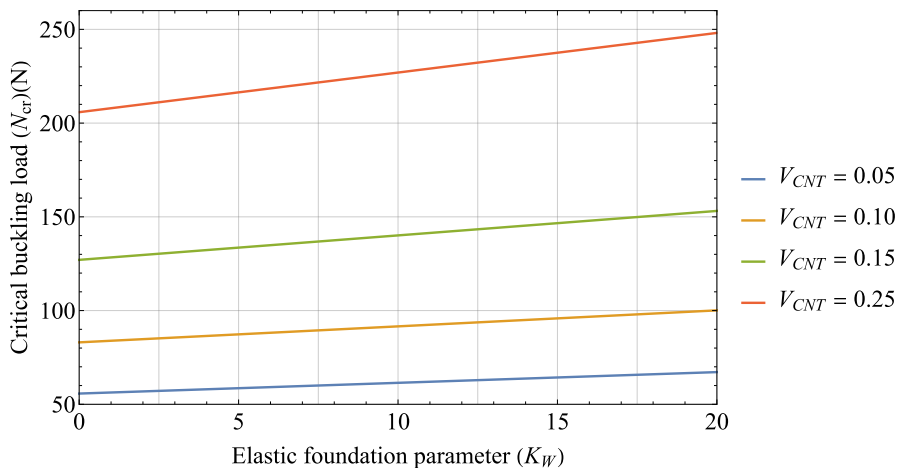| V_{CNT}	K_W								
	0	1	2	3	4	5	10	20	50
5%	55.728	56.300	56.872	57.445	58.017	58.589	61.451	67.175	84.347
10%	83.045	83.898	84.751	85.604	86.456	87.309	91.574	100.104	125.692
15%	127.050	128.355	129.659	130.964	132.269	133.574	140.099	153.148	192.296
25%	205.828	207.942	210.056	212.170	214.284	216.398	226.968	248.109	311.531

Figure 6. N_{cr} values of long CNT reinforced nanobeam for different K_W and V_{CNT} parameters

When Tables 5-6 and Figures 5-6 are examined, it can be understood that the increase in CNT volume fractions increases the critical buckling loads. This increase is slightly higher for long CNT reinforced nanobeams. As a result of increasing the V_{CNT} value at different K_W values, the proportional increase in the critical buckling

load does not change. In other words, regardless of the K_W value, the change in the V_{CNT} value affects the critical buckling load strength proportionally in the same way. The same goes for vice versa; i.e., regardless of the V_{CNT} value, the change in the K_W value affects the critical buckling load strength proportionally in the same way. When one of the parameters is kept constant and the other parameter is increased equally in both cases, the V_{CNT} parameter increases the critical buckling load strength more than the K_W parameter.

Tables 7-8 and Figures 7-8 show the effects of the length-to-thickness ratio of the CNT reinforced nanobeams and different CNT volume fractions on the buckling behavior of short and long CNT reinforced nanobeams. $\mu = 1$ and $K_W = 20$ values are used during the analysis.

Table 7. N_{cr} values (N) of short CNT reinforced nanobeam for different L/h and V_{CNT} values

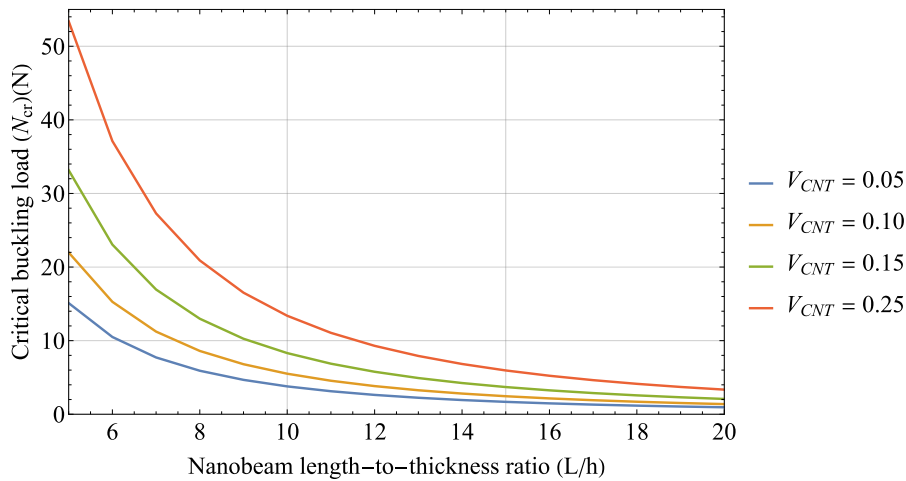| V_{CNT}	L/h			
	5	10	20	50
5%	15.1021	3.7848	0.9468	0.1515
10%	21.9754	5.5073	1.3777	0.2205
15%	33.1607	8.3105	2.0789	0.3327
25%	53.3970	13.3820	3.3476	0.5357

Figure 7. N_{cr} values of short CNT reinforced nanobeam for different L/h and V_{CNT} values

Table 8. N_{cr} values (N) of long CNT reinforced nanobeam for different L/h and V_{CNT} values

V_{CNT}	L/h			
	5	10	20	50
5%	267.9336	67.1477	16.7972	2.6880
10%	399.2720	100.0628	25.0311	4.0057
15%	610.8443	153.0856	38.2949	6.1282
25%	989.6034	248.0076	62.0400	9.9281

When Tables 7-8 and Figures 7-8 are analyzed, it is seen that the critical buckling load decreases as the length-to-thickness ratio of the nanobeam increases. This indicates that longer and thinner beams are more prone to buckling. In addition, according to the Euler-Bernoulli beam theory, the critical buckling load depends primarily on the flexural rigidity and length of the beam. In particular, the critical buckling load is inversely proportional to the length of the beam. Therefore, as the L/h ratio increases (i.e., L increases), the critical buckling load decreases rapidly.
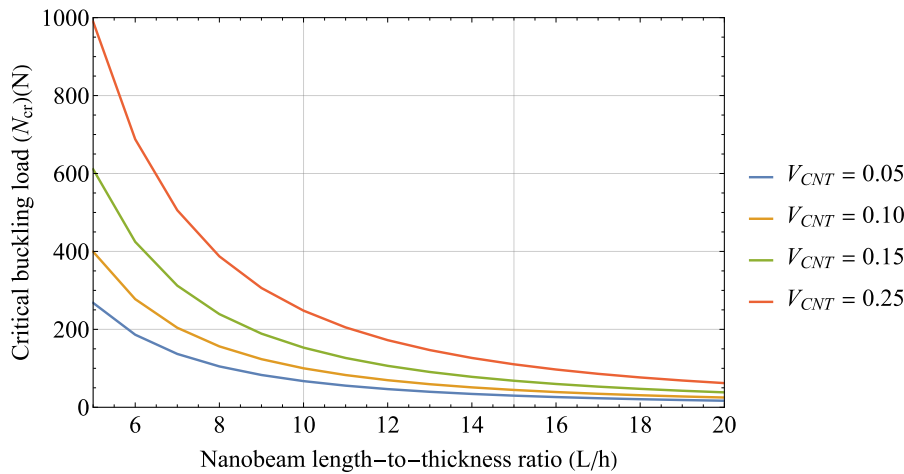
Figure 8. N_{cr} values of long CNT reinforced nanobeam for different L/h and V_{CNT} values

4. Conclusion

This study investigates the buckling behavior of short and long CNT reinforced nanobeams resting on elastic foundations. The effects on the critical buckling load are evaluated by considering various parameters such as short or long CNT reinforcement, CNT volume fraction, nonlocal parameter, elastic foundation parameter and length-to-thickness ratio of the nanobeam.

The results showed that an increase in the CNT volume fraction significantly increases the buckling strength of the nanobeam. CNT reinforcement strengthens the nanobeams' buckling strength, leading to higher critical buckling loads. CNT volume fraction is the most crucial parameter affecting buckling strength. This effect is observed for both short and long CNT reinforcements. The critical buckling loads of long CNT reinforced nanobeams are higher than those of short CNT reinforced nanobeams. This reveals that long CNTs contribute more to the mechanical performance of the nanobeam.

One of the most important results of this study is that the nonlocal parameter does not practically affect the buckling strength. Therefore, there is no need to use the nonlocal elasticity theory in mathematical modeling, which leads to a more complex formulation.

The elastic foundation parameter is another critical factor affecting the buckling behavior of the nanobeam. A significant increase in the critical buckling load was observed with the rise of the K_W value. This result shows that the nanobeam exhibits a stronger buckling strength when placed on the elastic foundation. The elastic foundation parameter strengthens the structural integrity of the nanobeam and increases its resistance to buckling.

Finally, it is found that the critical buckling load decreases as the length-to-thickness ratio of the nanobeam increases. This result indicates that longer and thinner nanobeams are more prone to buckling. As the length-to-thickness ratio of the nanobeam increases, the structure's stability decreases, negatively affecting the buckling resistance. This parameter, together with the CNT volume fraction parameter, is the parameter that most affects the buckling strength of the nanobeam. Since the buckling strength will be significantly reduced, especially in long, thin beams, this negative effect can be mitigated by using a high CNT volume fraction.

In the design of nanobeams resting on a Winkler-type elastic foundation, particular attention should be paid to the CNT volume fraction and length-to-thickness ratio parameters.

Author contribution

The authors contributed to all sections. The authors read and approved the last version of the manuscript.

Declaration of ethical code

The authors of this article declare that the material and the methods used in this study do not require ethics committee approval and/or special legal permission.

Conflicts of interest

The authors declare that there is no conflict of interest.

References

Aifantis, E. C. (1999). Strain gradient interpretation of size effects. *International Journal of Fracture*, *95*(1–4), 299–314. https://doi.org/10.1007/978-94-011-4659-3_16

Aria, A. I., & Friswell, M. I. (2019). A nonlocal finite element model for buckling and vibration of functionally graded nanobeams. Composites Part B: Engineering, 166, 233–246. https://doi.org/10.1016/j.compositesb.2018.11.071

Arshid, E., Arshid, H., Amir, S. & Mousavi, S. B. (2021). Free vibration and buckling analyses of FG porous sandwich curved microbeams in thermal environment under magnetic field based on modified couple stress theory. *Archives of Civil and Mechanical Engineering*, *21*(1), 6. https://doi:10.1007/s43452-020-00150-x

Ashrafi, B., Hubert, P. & Vengallatore, S. (2006). Carbon nanotube-reinforced composites as structural materials for microactuators in microelectromechanical systems. *Nanotechnology*, *17*(19), 4895-4903. https://doi:10.1088/0957-4484/17/19/019

Balasubramanian, K. & Burghard, M. (2005). Chemically functionalized carbon nanotubes. *Small*, *1 2*(2), 180-92. https://doi:10.1002/SMLL.200400118

Baughman, R. H., Zakhidov, A. A. & De Heer, W. A. (2002). Carbon Nanotubes--the Route Toward Applications. *Science*, *297*(5582), 787-792. https://doi:10.1126/SCIENCE.1060928

Bentrar, H., Chorfi, S. M., Belalia, S. A., Tounsi, A., Ghazwani, M. H., & Alnujaie, A. (2023). Effect of porosity distribution on free vibration of functionally graded sandwich plate using the P-version of the finite element method. *Structural Engineering and Mechanics*, *88*(6), 551–567. https://doi.org/10.12989/sem.2023.88.6.551

Belarbi, M.-O., Houari, M.-S.-A., Daikh, A. A., Garg, A., Merzouki, T., Chalak, H. D., & Hirane, H. (2021). Nonlocal finite element model for the bending and buckling analysis of functionally graded nanobeams using a novel shear deformation theory. Composite Structures, 264, 113712. https://doi.org/10.1016/j.compstruct.2021.113712

Casafont, M., Marimon, F., & Pastor, M. M. (2009). Calculation of pure distortional elastic buckling loads of members subjected to compression via the finite element method. *Thin-Walled Structures*, *47*(6–7), 701–729. https://doi.org/10.1016/j.tws.2008.12.001

Chi Tho, N., van Thom, D., Hong Cong, P., Zenkour, A. M., Hong Doan, D., & van Minh, P. (2023). Finite element modeling of the bending and vibration behavior of three-layer composite plates with a crack in the core layer. *Composite Structures*, *305*, 116529. https://doi.org/10.1016/j.compstruct.2022.116529

Civalek, Ö., & Numanoğlu, H. M. (2020). Nonlocal finite element analysis for axial vibration of embedded love–bishop nanorods. International Journal of Mechanical Sciences, 188, 105939. https://doi.org/10.1016/j.ijmecsci.2020.105939

Civalek, Ö., Uzun, B., Yaylı, M. Ö., & Akgöz, B. (2020a). Size-dependent transverse and longitudinal vibrations of embedded carbon and silica carbide nanotubes by nonlocal finite element method. The European Physical Journal Plus, 135(4), 381. https://doi.org/10.1140/epjp/s13360-020-00385-w

Civalek, Ö., Uzun, B. & Yaylı, M. Ö. (2020b). Stability analysis of nanobeams placed in electromagnetic field using a finite element method. *Arabian Journal of Geosciences*, *13*(21), 1165. https://doi:10.1007/s12517-020-06188-8

Dai, K. Y., & Liu, G. R. (2007). Free and forced vibration analysis using the smoothed finite element method (SFEM). *Journal of Sound and Vibration*, *301*(3–5), 803–820. https://doi.org/10.1016/j.jsv.2006.10.035

Demir, C., Mercan, K., Numanoglu, H. M., & Civalek, O. (2018). Bending Response of Nanobeams Resting on Elastic Foundation. Journal of Applied and Computational Mechanics, 4(2), 105–114. https://doi.org/10.22055/jacm.2017.22594.1137

Eltaher, M. A., Alshorbagy, A. E., & Mahmoud, F. F. (2013). Vibration analysis of Euler–Bernoulli nanobeams by using finite element method. Applied Mathematical Modelling, 37(7), 4787–4797. https://doi.org/10.1016/j.apm.2012.10.016

Eringen, A. C. (1967). Theory of micropolar plates. *Zeitschrift Für Angewandte Mathematik Und Physik ZAMP 1967 18:1*, *18*(1), 12–30. https://doi.org/10.1007/BF01593891

Esawi, A. M. K. & El Borady, M. A. (2008). Carbon nanotube-reinforced aluminium strips. *Composites Science and Technology*, *68*(2), 486-492. https://doi:10.1016/J.COMPSCITECH.2007.06.030

Fattahi, A. M. & Safaei, B. (2017). Buckling analysis of CNT-reinforced beams with arbitrary boundary conditions. *Microsystem Technologies*, *23*(10), 5079-5091. https://doi:10.1007/s00542-017-3345-5

Feng, Y., Kowalsky, M. J., & Nau, J. M. (2015). Finite-Element Method to Predict Reinforcing Bar Buckling in RC Structures. *Journal of Structural Engineering*, *141*(5). https://doi.org/10.1061/(ASCE)ST.1943-541X.0001048

Gurtin, M. E., Weissmüller, J., & Larché, F. (1998). A general theory of curved deformable interfaces in solids at equilibrium. *Philosophical Magazine A*, *78*(5), 1093–1109. https://doi.org/10.1080/01418619808239977

Kafkas, U. (2024). Değiştirilmiş Gerilme Çifti Teorisi ile Gözenekli Fonksiyonel Derecelendirilmiş Konsol Nanokirişlerin Statik Analizi. Uludağ University Journal of The Faculty of Engineering, 29(2), 393–412. https://doi.org/10.17482/uumfd.1459934

Kahya, V., & Turan, M. (2017). Bending of Laminated Composite Beams by a Multi-Layer Finite Element Based on a Higher-Order Theory. Acta Physica Polonica A, 132(3), 473–475. https://doi.org/10.12693/APhysPolA.132.473

Karamanli, A., & Vo, T. P. (2022). Finite element model for free vibration analysis of curved zigzag nanobeams. Composite Structures, 282, 115097. https://doi.org/10.1016/J.COMPSTRUCT.2021.115097

Lal, A. & Markad, K. (2019). Thermo-Mechanical Post Buckling Analysis of Multiwall Carbon Nanotube-Reinforced Composite Laminated Beam under Elastic Foundation. *Curved and Layered Structures*, *6*(1), 212-228. https://doi:10.1515/CLS-2019-0018

Lam, D. C. C., Yang, F., Chong, A. C. M., Wang, J., & Tong, P. (2003). Experiments and theory in strain gradient elasticity. *Journal of the Mechanics and Physics of Solids*, *51*(8), 1477–1508. https://doi.org/10.1016/S0022-5096(03)00053-X

Lim, C. W., Zhang, G., & Reddy, J. N. (2015). A higher-order nonlocal elasticity and strain gradient theory and its applications in wave propagation. *Journal of the Mechanics and Physics of Solids*, *78*, 298–313. https://doi.org/10.1016/J.JMPS.2015.02.001

Mesbah, A., Belabed, Z., Amara, K., Tounsi, A., Bousahla, A. A., & Bourada, F. (2023). Formulation and evaluation a finite element model for free vibration and buckling behaviours of functionally graded porous (FGP) beams. *Structural Engineering and Mechanics*, *86*(3), 291–309. https://doi.org/10.12989/sem.2023.86.3.291

Mindlin, R. D. (1965). Second gradient of strain and surface-tension in linear elasticity. *International Journal of Solids and Structures*, *1*(4), 417–438. https://doi.org/10.1016/0020-7683(65)90006-5

Motevalli, B., Montazeri, A., Tavakoli-Darestani, R. & Rafii-Tabar, H. (2012). Modeling the buckling behavior of carbon nanotubes under simultaneous combination of compressive and torsional loads. *Physica E-low-dimensional Systems & Nanostructures*, *46*, 139-148. https://doi:10.1016/J.PHYSE.2012.09.006

Namilae, S. & Chandra, N. (2006). Role of atomic scale interfaces in the compressive behavior of carbon nanotubes in composites. *Composites Science and Technology*, *66*(13), 2030-2038. https://doi:10.1016/j.compscitech.2006.01.009

Phadikar, J. K. & Pradhan, S. C. (2010). Variational formulation and finite element analysis for nonlocal elastic nanobeams and nanoplates. *Computational Materials Science*, *49*(3), 492-499. https://doi:10.1016/j.commatsci.2010.05.040

Pham, Q.-H., Tran, V. K., & Nguyen, P.-C. (2022). Hygro-thermal vibration of bidirectional functionally graded porous curved beams on variable elastic foundation using generalized finite element method. *Case Studies in Thermal Engineering*, *40*, 102478. https://doi.org/10.1016/j.csite.2022.102478

Popov, V. N., Van Doren, V. E. & Balkanski, M. (2000). Elastic properties of crystals of single-walled carbon nanotubes. *Solid State Communications*, *114*(7), 395-399. https://doi:10.1016/S0038-1098(00)00070-3

Pouresmaeeli, S. & Fazelzadeh, S. A. (2017). Uncertain Buckling and Sensitivity Analysis of Functionally Graded Carbon Nanotube-Reinforced Composite Beam. *International Journal of Applied Mechanics*, *09*(05), 1750071. https://doi:10.1142/S1758825117500715

Pradhan, S. C. & Reddy, G. K. (2011). Buckling analysis of single walled carbon nanotube on Winkler foundation using nonlocal elasticity theory and DTM. *Computational Materials Science*, *50*(3), 1052-1056. https://doi:10.1016/J.COMMATSCI.2010.11.001

Reddy, J. N. (2002). *Energy Principles and Variational Methods in Applied Mechanics* (2nd ed.). John Wiley and Sons.

Reddy, J. N., Nampally, P., & Srinivasa, A. R. (2020). Nonlinear analysis of functionally graded beams using the dual mesh finite domain method and the finite element method. *International Journal of Non-Linear Mechanics*, *127*, 103575. https://doi.org/10.1016/j.ijnonlinmec.2020.103575

Setoodeh, A. R., Derahaki, M. & Bavi, N. (2015). DQ thermal buckling analysis of embedded curved carbon nanotubes based on nonlocal elasticity theory. *Latin American Journal of Solids and Structures*, *12*(10), 1901-1917. https://doi:10.1590/1679-78251894

Shen, H.-S. (2009). Nonlinear bending of functionally graded carbon nanotube-reinforced composite plates in thermal environments. *Composite Structures*, *91*(1), 9-19. https://doi:10.1016/j.compstruct.2009.04.026

Song, W., Deng, Z., Wu, H., & Zhan, Y. (2022). Extended finite element modeling of hot mix asphalt based on the semi-circular bending test. *Construction and Building Materials*, *340*, 127462. https://doi.org/10.1016/j.conbuildmat.2022.127462

Suhr, J., Koratkar, N., Keblinski, P. & Ajayan, P. (2005). Viscoelasticity in carbon nanotube composites. *Nature Materials*, *4*(2), 134-137. https://doi:10.1038/nmat1293

Taghizadeh, M., Ovesy, H. R. & Ghannadpour, S. A. M. (2016). Beam Buckling Analysis by Nonlocal Integral Elasticity Finite Element Method. *International Journal of Structural Stability and Dynamics*, *16*(06), 1550015. https://doi:10.1142/S0219455415500157

Thang, P. T. (2019). Geometrically nonlinear buckling analysis of functionally graded carbon nanotube reinforced cylindrical panels resting on Winkler–Pasternak elastic foundation. *Proceedings of the Institution of Mechanical Engineers, Part C: Journal of Mechanical Engineering Science*, *233*(2), 702-712. https://doi:10.1177/0954406218760957

Toupin, R. (1962). Elastic materials with couple-stresses. *Archive for Rational Mechanics and Analysis*, *11*(1), 385–414. https://doi.org/10.1007/BF00253945

Tuna, M., & Kirca, M. (2017). Bending, buckling and free vibration analysis of Euler-Bernoulli nanobeams using Eringen's nonlocal integral model via finite element method. Composite Structures, 179, 269–284. https://doi.org/10.1016/j.compstruct.2017.07.019

Turan, M., & Hacıoğlu, M. İ. (2022). Buckling Analysis of Functionally Graded Beams Using the Finite Element Method. Erzincan Üniversitesi Fen Bilimleri Enstitüsü Dergisi, 15(Special Issue I), 98–109. https://doi.org/10.18185/erzifbed.1199454

Turan, M., & Hacıoğlu, M. İ. (2023). Yüksek mertebe sonlu eleman modeliyle fonksiyonel derecelendirilmiş kirişlerin serbest titreşim ve statik analizi. Gümüşhane Üniversitesi Fen Bilimleri Enstitüsü Dergisi. https://doi.org/10.17714/gumusfenbil.1185301

Turan, M., & Kahya, V. (2018). Fonksiyonel Derecelendirilmiş Kirişlerin Serbest Titreşim Analizi. Karadeniz Fen Bilimleri Dergisi, 8(2), 119–130. https://doi.org/10.31466/kfbd.453833

Turan, M., & Kahya, V. (2021). Fonksiyonel derecelendirilmiş sandviç kirişlerin Navier yöntemiyle serbest titreşim ve burkulma analizi. Gazi Üniversitesi Mühendislik Mimarlık Fakültesi Dergisi, 36(2), 743–758. https://doi.org/10.17341/gazimmfd.599928

Uhm, T., & Youn, S. (2009). T-spline finite element method for the analysis of shell structures. *International Journal for Numerical Methods in Engineering*, *80*(4), 507–536. https://doi.org/10.1002/nme.2648

Uzun, B., Kafkas, U., & Yaylı, M. Ö. (2021). Free vibration analysis of nanotube based sensors including rotary inertia based on the Rayleigh beam and modified couple stress theories. Microsystem Technologies, 27(5), 1913–1923. https://doi.org/10.1007/s00542-020-04961-z

Uzun, B., Numanoglu, H., & Civalek, O. (2018). Free vibration analysis of BNNT with different cross-Sections via nonlocal FEM. Journal of Computational Applied Mechanics, 49(2), 252–260. https://doi.org/10.22059/jcamech.2018.266789.328

Uzun, B., & Yaylı, M. Ö. (2022). A Finite Element Solution for Bending Analysis of a Nanoframe using Modified Couple Stress Theory. International Journal of Engineering and Applied Sciences, 14(1), 1–14. https://doi.org/10.24107/ijeas.1064690

Uzun, B., Yaylı, M. Ö., & Deliktaş, B. (2020). Free vibration of FG nanobeam using a finite-element method. Micro & Nano Letters, 15(1), 35–40. https://doi.org/10.1049/mnl.2019.0273

Wang, Q., Varadan, V. K., & Quek, S. T. (2006). Small scale effect on elastic buckling of carbon nanotubes with nonlocal continuum models. *Physics Letters A*, *357*(2), 130–135. https://doi.org/10.1016/j.physleta.2006.04.026

Wang, Q., Liew, K. M., He, X. Q. & Xiang, Y. (2007). Local buckling of carbon nanotubes under bending. *Applied Physics Letters*, *91*(9). https://doi:10.1063/1.2778546

Wattanasakulpong, N. & Ungbhakorn, V. (2013). Analytical solutions for bending, buckling and vibration responses of carbon nanotube-reinforced composite beams resting on elastic foundation. *Computational Materials Science*, *71*, 201-208. https://doi:10.1016/J.COMMATSCI.2013.01.028

Wu, C.-P. & Yu, J.-J. (2019). A review of mechanical analyses of rectangular nanobeams and single-, double-, and multi-walled carbon nanotubes using Eringen's nonlocal elasticity theory. *Archive of Applied Mechanics*, *89*(9), 1761-1792. https://doi:10.1007/s00419-019-01542-z

Yang, F., Chong, A. C. M., Lam, D. C. C., & Tong, P. (2002). Couple stress based strain gradient theory for elasticity. *International Journal of Solids and Structures*, *39*(10), 2731–2743. https://doi.org/10.1016/S0020-7683(02)00152-X

Yaylacı, M., Yaylacı, E. U., Özdemir, M. E., Öztürk, Ş., & Sesli, H. (2023). Vibration and buckling analyses of FGM beam with edge crack: Finite element and multilayer perceptron methods. *Steel and Composite Structures*, *46*(4), 565–575. https://doi.org/10.12989/scs.2023.46.4.565

Yaylı, M.Ö. (2015). Buckling Analysis of a Rotationally Restrained Single Walled Carbon Nanotube. *Acta Physica Polonica A*, *127*(3), 678-683. https://doi:10.12693/APhysPolA.127.678

Yaylı, M. Ö. (2017). Buckling analysis of a cantilever single-walled carbon nanotube embedded in an elastic medium with an attached spring. *Micro & Nano Letters*, *12*(4), 255-259. https://doi:10.1049/mnl.2016.0662

Yaylı, M. Ö. (2019). Stability analysis of a rotationally restrained microbar embedded in an elastic matrix using strain gradient elasticity. *Curved and Layered Structures*, *6*(1), 1-10. https://doi:10.1515/cls-2019-0001

Zhu, S., Dong, R., Liu, Z., Liu, H., Lu, Z., & Guo, Y. (2024). A finite element method study of the effect of vibration on the dynamic biomechanical response of the lumbar spine. *Clinical Biomechanics*, *111*, 106164. https://doi.org/10.1016/j.clinbiomech.2023.106164